

Soft probes of p+Pb and Pb+Pb collisions in the ATLAS experiment at the LHC

S. Radhakrishnan for the ATLAS collaboration.

Department of Physics, Stony Brook University, NY, USA

Abstract. Collective flow and azimuthal correlation measurements of particles in the p_T region $\lesssim 10$ GeV provide valuable information in constraining the initial conditions and expansion dynamics of the system produced in heavy-ion collisions. ATLAS collaboration has recently measured correlations between flow harmonics in Pb+Pb collisions at $\sqrt{s_{NN}} = 2.76$ TeV, using an event-shape selection procedure, and has separated the components arising from linear and non-linear hydrodynamic evolution in higher order harmonics (v_4 and v_5). A brief overview of these results are presented in these proceedings. Recently, azimuthal correlations extending to large pseudorapidity differences (“ridge”), similar to that seen in heavy-ion collisions, was observed in p+Pb collisions at LHC. These proceedings also present a measurement of the Fourier harmonics associated with the ridge correlations (v_1 to v_5) in p+Pb collisions at $\sqrt{s_{NN}} = 5.02$ TeV by ATLAS collaboration. The results are compared with v_n in Pb+Pb collisions at $\sqrt{s_{NN}} = 2.76$ TeV with similar event multiplicities. Reasonable agreement is observed after accounting for the difference in the average p_T of particles produced in the two collision systems, consistent with a recent hydrodynamic calculation.

1. Introduction

The particles produced in heavy-ion collisions at RHIC and LHC show azimuthal anisotropy that extend over large pseudorapidity (η) [1, 2]. In AA collisions these long-range correlations are well described by a hydrodynamic expansion resulting from the anisotropic initial density distribution [3, 4]. The azimuthal anisotropy in particle production is often expanded in a Fourier series, $\frac{dN}{d\phi} \sim 1 + \sum_{n=1}^{\infty} 2v_n \cos(n(\phi - \Psi_n))$. The second and third harmonics in the Fourier expansion arise from a linear response to the corresponding initial eccentricities, ϵ_n , i.e $v_n \propto \epsilon_n$ [5]. However higher-order harmonics contain non-linear contributions from lower-order harmonics [5, 6]. Using an event-shape selection procedure, ATLAS collaboration has measured the correlations between flow harmonics in Pb+Pb collisions at $\sqrt{s_{NN}} = 2.76$ TeV. The correlation between higher and lower-order harmonics show non-linear correlations, consistent with expectations from hydrodynamics. The linear and non-linear components are separated from the measured correlations for different centrality intervals. A brief discussion of these results are presented in these proceedings.

Recently, azimuthal correlations extending to large pseudorapidity differences (referred to as “ridge”), similar to that observed in heavy-ion collisions, was observed in p+Pb collisions at LHC [7, 8, 9] and d+Au collisions at RHIC [10]. The theoretical understanding of the origin of these correlations is still a matter of debate [11, 12]. ATLAS collaboration has done a detailed measurement of the first five Fourier harmonics ($v_1 - v_5$) associated with the ridge correlations in p+Pb collisions at $\sqrt{s_{NN}} = 5.02$ TeV. These proceedings discuss the ATLAS v_n results in p+Pb collisions. A comparison between v_n from p+Pb collisions and Pb+Pb collisions at $\sqrt{s_{NN}}$



= 2.76 TeV with similar event multiplicity is also included. Reasonable agreements are observed after accounting for the difference in the average p_T of particles produced in the two collision systems, consistent with a recent hydrodynamic calculation, thus suggesting a similar or perhaps common origin of these correlations in both systems.

2. Flow correlations in Pb+Pb collisions

Correlation between flow harmonics in heavy-ion collisions can be studied using an event-shape analysis. The event-shape selection is done using the transverse energy (E_T) distribution in the ATLAS [13] forward calorimeter (FCal) in $3.3 < |\eta| < 4.9$. For each event, the energy distribution is expanded in a Fourier series, $2\pi \frac{dE_T}{d\phi} = (\sum E_T)(1 + 2 \sum_{n=1}^{\infty} q_n \cos(n(\phi - \psi_n)))$. The reduced flow vector, q_n , represents the E_T weighted observed flow coefficients. In each centrality class, events are classed into different ellipticity bins according to the value of the observed elliptic flow, q_2 . The v_n values are then calculated for each of these q_2 classes using tracks in the Inner Detector (ID, $|\eta| < 2.5$), using a two-particle correlation method.

The left panel in Figure 1 shows the v_4 values measured in the ID, as a function of the v_2 values measured in the ID for different q_2 classes. The results for different centrality classes are shown. The observed non-linear correlation between v_4 and v_2 is found to be well described by a two component fit, motivated by hydrodynamics [5], of the form $v_4 = \sqrt{c_0^2 + (c_1 v_2^2)^2}$. The middle panel shows the extracted linear ($v_n^L = c_0$) and non-linear components ($v_n^{NL} = \sqrt{v_n^2 - c_0^2}$), for $n = 4$, as a function of the number of participants. The values from a similar decomposition using the results from event-plane correlation measurements [14] are also shown. Good agreement can be seen between both, suggesting that the correlations between flow magnitudes arise from the correlations between the flow angles. Right panel shows a similar decomposition for v_5 , from a fit of the form $v_5 = \sqrt{c_0^2 + (c_1 v_2 v_3)^2}$ to the measured correlation between v_5 and v_2 . More results related to the analysis along with a detailed description of the procedure and systematics can be found elsewhere [15].

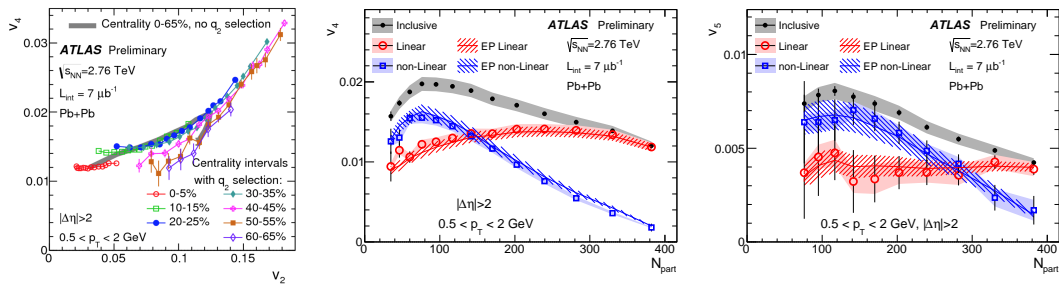


Figure 1. (Left) Correlation between v_2 and v_4 , both measured in $0.5 < p_T < 2$ GeV, for different centrality intervals. The data points in each centrality interval correspond to different q_2 bins. (Middle) N_{part} dependence of v_4 and the extracted linear and non-linear components associated with it. Also shown are the linear and non-linear components calculated from event-plane correlations. (Right) Similar plot for v_5 . Error bars and shaded bands represent statistical and systematic uncertainties, respectively. [15]

3. Ridge in p +Pb collisions

The long-range correlations in p +Pb are studied using two-particle correlation constructed using the charged particle tracks reconstructed in the ID. A recoil subtraction procedure, similar to that described in [9], is applied at the per-trigger yield level by subtracting the per-trigger yield above uncorrelated pairs in a “peripheral” event class – defined as having $E_T < 10$ GeV in the FCal on the Pb-going side. The recoil subtracted distribution is then expanded in a Fourier

series, and the two particle harmonic coefficients $v_{n,n}$ in the expansion are used to compute the single particle coefficients v_n , assuming factorization: $v_n(p_T^a) = v_{n,n}(p_T^a, p_T^b) / \sqrt{v_{n,n}(p_T^b, p_T^b)}$. A detailed description of the analysis procedure and systematic uncertainties along with a complete set of results can be found in [16].

The v_n values extracted from the subtracted distribution, for $n = 2, 3, 4$ and 5 , as a function of the transverse momentum are shown in the left panel of Figure 2, for events with $220 \leq N_{\text{ch}}^{\text{rec}} < 260$. The v_n values increase with p_T in the low p_T region, reach a maximum around $3 - 5$ GeV and then decrease with further increase in p_T , but remain positive in the measured range. This is similar to the p_T dependence of v_n harmonics measured in heavy-ion collisions [17]. The magnitude of v_n is found to decrease with increasing harmonic number n . The second panel of Figure 2 shows the first order harmonic, v_1 , as a function of p_T^a . The values are obtained assuming factorization, but accounting for the sign change of v_1 at low p_T . Good agreements are found between the v_1 values extracted using three different p_T^b ranges. The v_1 is negative at low p_T , crosses zero ~ 1.5 GeV and then increase to 0.1 in the $4 - 6$ GeV range. A similar p_T dependence for v_1 (with $v_1(p_T)$ crossing zero ~ 1.1 GeV) was observed in Pb+Pb collisions at $\sqrt{s_{\text{NN}}} = 2.76$ TeV [17].

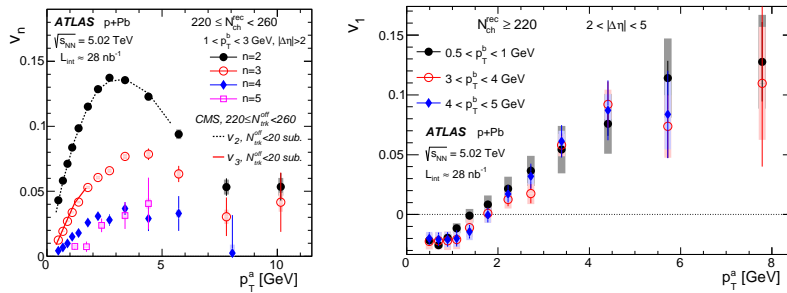


Figure 2. (Left) v_n for $n = 2-5$ as a function of p_T^a for associated particles in the range $1 < p_T^b < 3$ GeV and $2 < |\Delta\eta| < 5$ for events with $220 \leq N_{\text{ch}}^{\text{rec}} < 260$. (Right) v_1 as a function of p_T^a for different associated p_T selections for events with $220 \leq N_{\text{ch}}^{\text{rec}} < 260$. The error bars and shaded boxes represent the statistical and systematic uncertainties, respectively [16].

The left-panels of Figure 3 compares the v_n values from p +Pb collision in the event-activity class $220 \leq N_{\text{ch}}^{\text{rec}} < 260$ with those from Pb+Pb collisions in 55–60% centrality from [17]. The two event classes are selected such that they have similar efficiency corrected number of tracks with $p_T > 0.5$ GeV and $|\eta| < 2.5$. The larger v_2 values in Pb+Pb collisions can be attributed to the elliptic collision geometry of the Pb+Pb system, while the larger v_4 values could be due to the non-linear coupling between v_2 and v_4 in the collective expansion [15]. The v_3 data for Pb+Pb collisions are similar in magnitude to those in p +Pb collisions which could be expected if v_3 arises from density fluctuations in both systems. A scaling relation between the v_n of p +Pb and $v_n(p_T/K)$ in Pb+Pb systems should be proportional to each other at a given p_T , with $K = 1.25$ being the ratio of mean p_T in the two collision systems. The right panels of Figure 3 show the comparison between $v_n(p_T)$ in p +Pb and $v_n(p_T/K)$ in Pb+Pb. The $v_2(p_T/K)$ and $v_4(p_T/K)$ in Pb+Pb are also scaled vertically by an empirical factor of 0.66. The two sets of values are found to agree well with each other after the scaling of p_T axis.

4. Conclusions

Event-shape selection are used to measure correlations between flow harmonics and to separate linear and non-linear components in higher harmonics (v_4 and v_5). The linear and non-linear

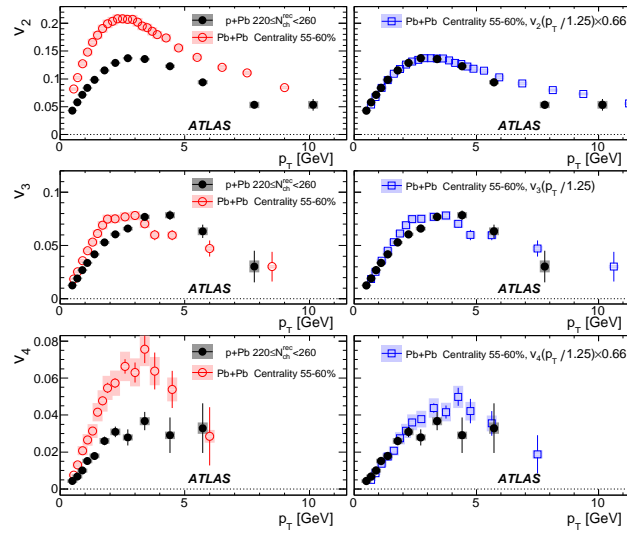


Figure 3. v_2 (top row), v_3 (middle row) and v_4 (bottom row) data compared between p +Pb collisions with $220 \leq N_{ch}^{rec} < 260$ in this analysis and Pb+Pb collisions in 55-60% centrality from [17]. Left column shows the original data with their statistical (error bars) and systematic uncertainties (shaded boxes). In right column, the same Pb+Pb data are rescaled horizontally by a constant factor of 1.25, and the v_2 and v_4 are also down-scaled by an empirical factor of 0.66 to match the p +Pb data [16].

components are extracted as function of centrality and show good agreement with the linear and non-linear components evaluated from event-plane correlation measurements. The first five Fourier harmonics associated with the ridge correlations in p +Pb collisions are measured. The v_n values show similar p_T dependence as the v_n from heavy-ion collisions. The $v_n(p_T)$ values from p +Pb collisions (for $n = 2, 3$ and 4) are compared to those from Pb+Pb collisions for event class with similar average multiplicity. After applying a scale factor of $K = 1.25$, that accounts for the difference of mean p_T in the two collision systems, the $v_n(p_T/K)$ from Pb+Pb is found to have similar shape as the $v_n(p_T)$ from p +Pb collisions. This could suggest that the long-range correlations in p +Pb and Pb+Pb systems are driven by similar dynamics.

5. References

- [1] Ackermann K *et al.* [STAR Collaboration], *Phys.Rev.Lett.* **86**, 402 (2001)
- [2] Aamodt K *et al.* [ALICE Collaboration], *Phys.Rev.Lett.* **107** (2011) 032301
- [3] Heinz U W and Snellings R, *Ann.Rev.Nucl.Part.Sci.* **63** (2013) 123
- [4] Alver B and Roland G, *Phys.Rev.C* **81** (2010) 054905
- [5] Gardim F G, Grassi F, Luzum M, and Ollitrault J-Y, *Phys.Rev.C* **85** (2012) 024908
- [6] Teaney D and Yan L, *Phys.Rev.C* **90** 024902
- [7] Abelev B *et al.* [ALICE Collaboration], *Phys.Lett.B* **719**, (2013) 29-41
- [8] ATLAS Collaboration, *Phys.Rev.Lett.* **110**, 182302 (2013)
- [9] CMS Collaboration, *Phys.Lett.B* **724** (2013) 213
- [10] Adare A *et al.* [PHENIX Collaboration], *Phys.Rev.C* **78** (2008) 014901
- [11] Bozek P, *Phys.Rev.C* **85** (2012) 014911
- [12] Dusling K and Venugopalan R, *Phys.Rev.D* **87** no. 5, (2013) 051502
- [13] ATLAS Collaboration, 2008 *JINST* **3** S08003
- [14] ATLAS Collaboration, *Phys.Rev.C*, **90** (2014) 024905.
- [15] ATLAS Collaboration, ATLAS-CONF-2014-022, <http://cds.cern.ch/record/1702980>
- [16] ATLAS Collaboration, *Phys.Rev.C* **90** 044906 (2014)
- [17] ATLAS Collaboration, *Phys.Rev.C* **86** (2012) 014907
- [18] Basar G and Teaney D, *Phys.Rev.C* **90** 054903